EXTRAPOLATING AERO DATA FROM A DEMONSTRATOR TO AN OPERATIONAL VEHICLE

J.M.A. Longo[(1)], H. Lüdeke[(1)], W. Kordulla[(2)], R. Molina[(2)]
[(1)] DLR, Institute of Aerodynamics and Flow Technology, Braunschweig, Germany
[(2)] ESA ESTEC, Noordwijk, The Netherlands

ABSTRACT

The study presents a numerical investigation for the SPHYNX re-entry vehicle performed by DLR under ESA contract. The current aero- and aero-thermodynamic study is carried out based on the solutions of the stationary Navier-Stokes equations. Several flow conditions derived from the flight trajectory are considered, in particular the portion comprised from 85 Km to 60 Km altitudes, i.e. Mach numbers from 28 to 14. All Navier-Stokes simulations are carried out for chemical non-equilibrium under laminar conditions. Fully and partially catalytic wall conditions are considered. The numerical solutions are assessed by grid convergence analysis and comparing the present data with available results for the X-38 vehicle. The study provides first positive evidences about the possibility to use an existing aerodynamic and/or aero-thermodynamic database to design a downsized or upsized vehicle which shall fly a different re-entry trajectory. Thus a verification of the applicability of X38 aerodynamic and aerothermodynamic databases is highlighted.

INTRODUCTION

Reusable or partially reusable space transportation systems are a possible alternative to the existing expendable launchers and re-entry capsules for economical access to/return from the orbital infrastructure, for both human space transportation and cargo transfer. The US Space Shuttle Orbiter is the only existing embodiment of a re-usable space transportation vehicle for humans as well as cargo. Based on a roughly 30 year old design this craft can, however, be re-used safely only after substantial and expensive refurbishments forbidding frequent flights.

Since ESA's Hermes development program, Europe has invested considerable efforts in the development of re-usable space vehicles. The most recent engagement was that one based on NASA's flight demonstrator X-38 of the Crew Return Vehicle (CRV) for the International Space Station [1, 2, 3]. The CRV in its X38 demonstrator implementation was to be a reusable craft, also serving the purposes of a test bed for recurrent operations of reusable systems. The European participation in the development of the X38 CRV demonstrator has provided continuity of its industrial activities in the field of both reusable transportation systems (if only for its re-entry component) and human space transportation, after the termination of the Hermes project and the successful completion of the ARD flight. Indeed, Europe has performed in the past several technologies development and vehicle system studies. It has also successfully flown the Atmospheric Re-entry Demonstrator, an Apollo-shaped capsule, using ablative TPS. The next step in technology demonstration is considered to validate an aerodynamically guided re-entry and advanced reusable thermal protection systems. For this purpose ESA is working at the definition of an atmospheric re-entry experimental vehicle, also in the relation to the expected application in the next operational systems. The actual operation of CRV space vehicles would have secured access to relevant information about potential benefits and caveats of reusable technologies at a moderate cost for Europe in partial fulfillment of its obligations concerning ISS exploitation costs.

Owing to the US decision to quit the CRV development and to drop the X-38 flight experiment, Europe cannot harvest the fruits of its investments by means of flight validation of its hard- and software developments. Within Europe there are, however, plans to carry out in-flight experimentation for re-entry lifting bodies as an intermediate step to larger demonstrators. In particular, to offer low-cost and low-risk flight opportunities the idea of a subscale vehicle based on the X-38 shape has been investigated by ESA. The vehicle, called SPHYNX (Subscale Precursor HYpersoNic X vehicle), has the shape of the X-38 lifting body, scaled down to 33%. It therefore should make use of the well-known aerodynamic and aerothermodynamic behavior of the X-38.

The objective of the present work is to reconsider the database, which has been established for the full-scale demonstrator X-38 by an ESA team and by the help of activities within DLR's technology program TETRA. This has to be done – actually in Europe for the first time known – in view of the requirements of a sub-scale re-entry vehicle. Owing to the reduced lengths and possibly different trajectories, the influence of viscosity and non-equilibrium effects has to be identified and clarified. This concerns also the possible changes to the existing database with respect to the effectiveness of the control surfaces. The results shall contribute to a reliable aero/aerothermodynamic database needed for in-flight experimentation with the sub-scale vehicle SPHYNX. The aero(thermo)dynamic analysis is carried out for selected flow conditions based on solutions of the steady Navier-Stokes equations.

NUMERICAL TOOLS

The computed flow solutions are carried out by means of the DLR Navier-Stokes code CEVCATS-N [4]. Here, only a brief description will be given. CEVCATS-N is a multi-block finite volume computational flow solver for the solution of the steady Euler and Navier-Stokes equations written in the integral form. The spatial discretization is done by a modified AUSM scheme that ensures high accuracy and sharp shock resolution. Second order accuracy is obtained by MUSCL extrapolation. The solution is advanced in time by means of a five-stage

Runge-Kutta scheme. For the present study, chemical non-equilibrium flows are computed by solving simultaneously the full Navier-Stokes equations and the species conservation laws for the chemical non-equilibrium. For calculations with wall catalysis the model of Bergemann [5] implemented by Brück [6] is used.

The computations for the SPHYNX configuration are done employing the same set of meshes used for the X-38 aerothermodynamic data base [7]. Those grids have been generated applying the DLR grid generator MegaCads [8]. Based on previous experience they have been designed parametrically and composed in a modular way. The X-38 grids allow a high resolution of the bow shock, wake and deflected flaps areas and have been successfully validated during ESA's X-38 step 2 activities.

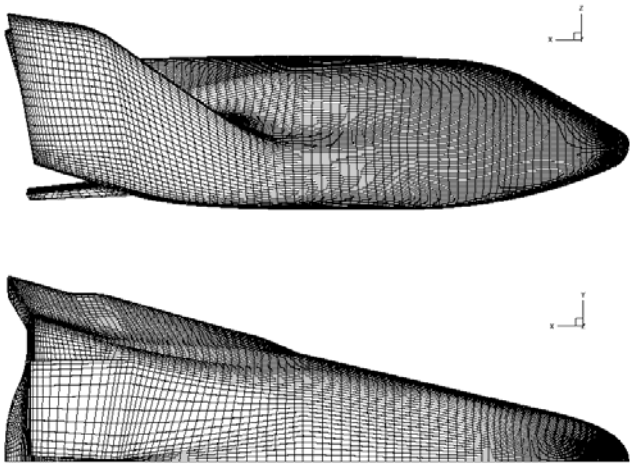

Fig. 1: Vehicle discretization with the standard grid.

For the present study three grid densities are used, called medium (M), standard (S) and refined grid (R). Each finer grid contains a number of points doubled in all directions with respect to the next coarser one. The standard grid is named fine grid level in previous X- 38 studies [7]. In all the cases, the first wall-normal spacing on the coarse level is y+< 0.4. Complete configurations have been simulated using a 1 million grid point's standard grid for symmetric configurations (only one half is considered for the computations as shows **Fig. 1**). The medium, standard and refined grid resolutions are shown in **Fig. 2**.

FLOW CONDITIONS

The free stream conditions for the simulations are shown in **Table 1**. A Mach number range from 14.6 to 26.8 at an angle of attack of 40 degrees is covered corresponding to trajectory points between 60 and 80 Km. For this trajectory segment influences of wall catalysis are highly important for the temperature distribution at the vehicle-nose. All flow conditions are treated laminar and computed with partial and full wall catalysis. Radiation adiabatic wall conditions with a radiation efficiency of e=0.85 are chosen.

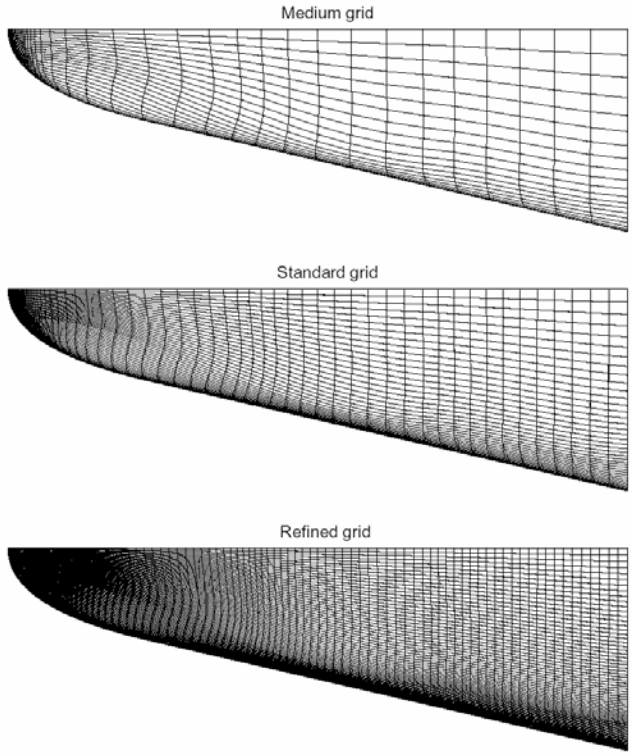

Fig. 2: Grid densities using for the present study. Top: medium grid (M), middle: standard grid (S), bottom: refined grid (R).

Table 1: Flow conditions considered for SPHYNX.

H [Km]	Ma	rho	Re/10^6	Tinf
80,0	26,8	18,50	0,030	199,0
75,0	24,5	41,00	0,058	208,0
70,0	21,0	82,80	0,101	220,0
60,0	14,6	309,60	0,240	247,0

RESULTS

Grid convergence studies carried out to check the suitability of the X-38 grids for the SPHYNX computations are done, for Ma = 21, using the three level grids. The other conditions are only simulated with the medium and the standard grids only. The temperature distribution at Ma = 21.0 resulting on the front part of the vehicle for the grid densities M, S and R is shown in **Fig. 3**. The pictures demonstrate a good convergence and a sufficient grid resolution when simulating the vehicle with the standard grid. The temperature at the nose (Tnose) is given for all the cases. The difference on the computed values between the medium and standard grids is in the range of 1.2% while for standard and refined grids the difference is only 0.8%. This is well inside the expected accuracy of a database. As previously mentioned, all calculations are carried out for full and partially catalytic wall conditions. **Figure 4** shows results for the same flow condition as in the previous figure but assuming the wall as fully catalytic. The maximum temperature at the nose is approx. 15% higher than when assuming partially catalytic wall. For this case as well as for all the other flow conditions, the results of the grid convergence study are quite satisfactory, although minor differences appear near the symmetry plane.

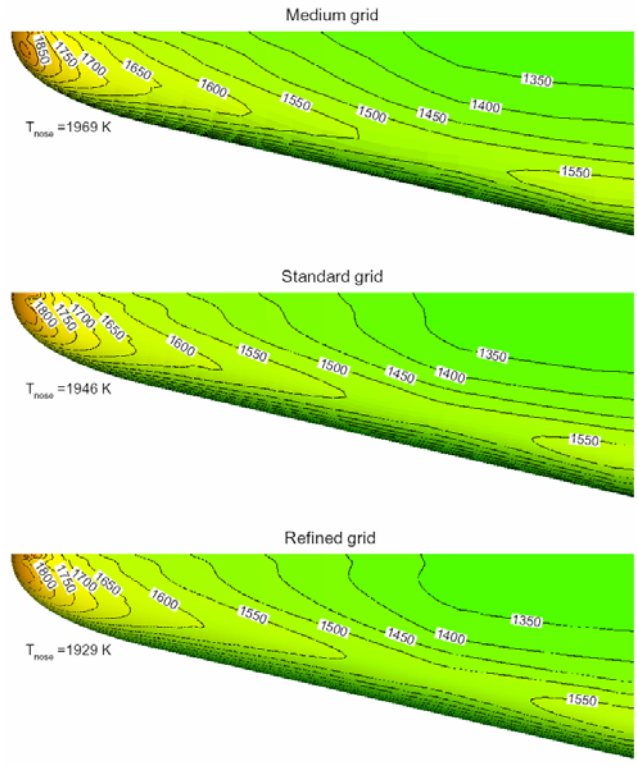

Fig. 3: Surface temperature distribution for Ma=21.0 assuming partially catalytic conditions.

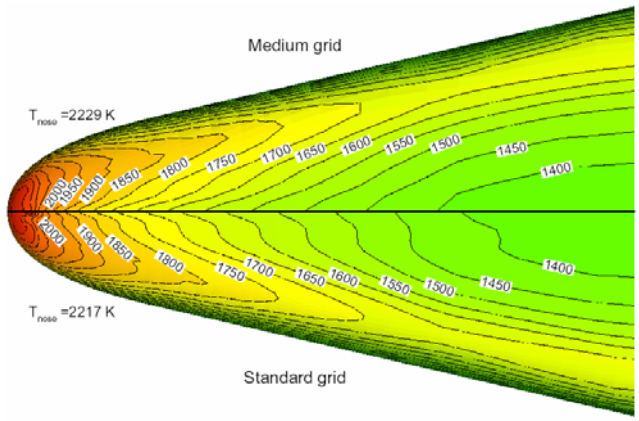

Fig. 4: Surface termperature distribution for Ma=21.0 assuming fully catalytic conditions.

On Figs. 5-7 the evolution of the temperature on different parts of the configuration as function of the flight altitude H are show. **Figure 5** demonstrates that at the nose the effect of wall catalysis reduces as the altitude increases and also that the influence of the grid density on the results is negligible. Indeed, at 75 Km altitude the differences in Tnose due to grid resolution are less than 1%. Also the temperature rise at this altitude, resulting from the wall treatment, decreases to 12% in comparison with the already mentioned 15% for 70 Km; a tendency that continues up to 80Km. At the configuration middle length, either windward side (**Fig. 6**) or leeward side (**Fig. 7**) the influence of wall catalysis is markedly lower than at the nose. In all the cases, the computed temperatures assuming fully catalytic walls are globally higher than the temperatures obtained for partially catalytic walls.

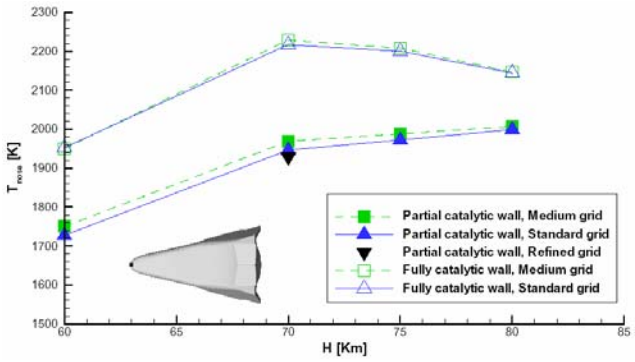

Fig. 5: Evolution of the stagnation temperature as a function of wall conditions, grid density and flight altitude.

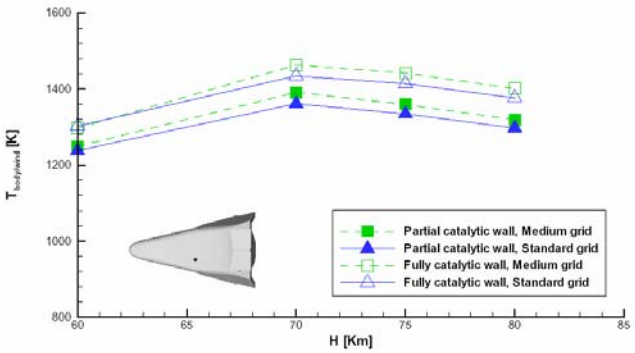

Fig. 6: Evolution of the windward side temperature as a function of wall conditions, grid density and flight altitude.

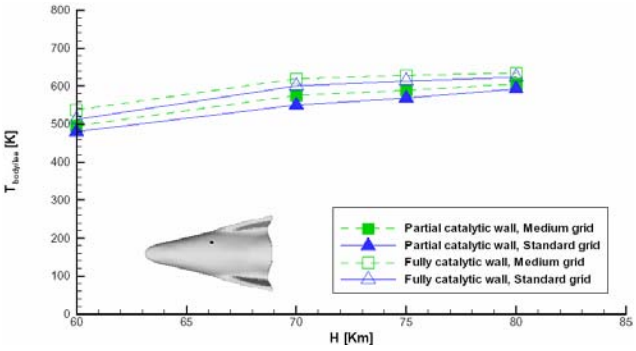

Fig. 7: Evolution of the leeward side temperature as a function of wall conditions, grid density and flight altitude.

Figure 8 compares the results obtained at the same flow condition for the SPHYNX vehicle and for the X-38 configuration using two grid densities (medium and standard). As expected, the X-38 exhibits lower stagnation temperature due to the larger nose radius and therefore lower overall temperature downstream the stagnation point but both configurations exhibit the same temperature gradient between nose and tail. With respect to the impact of the grid density on the results for the aft part of the configuration, higher differences than those reported for the front part appear for both vehicles in particular in the flap region due to the grid resolution tends to be coarser there. The evolution of the temperature on a mid point of the flap as function of the flight altitude H for the SPHYNX (in the figure indicated as vehicle scale

factor 1) and for the X-38 configuration (vehicle scale factor 3) is shown in **Fig. 9**. The behavior of the flap temperature is the same for both configurations, i.e. a monotonously decreasing with altitude with almost the same gradient. Also while qualitative the trend is the same with both grid resolutions, it turns out the medium grid provides insufficient resolution to resolve the flow around the flap.

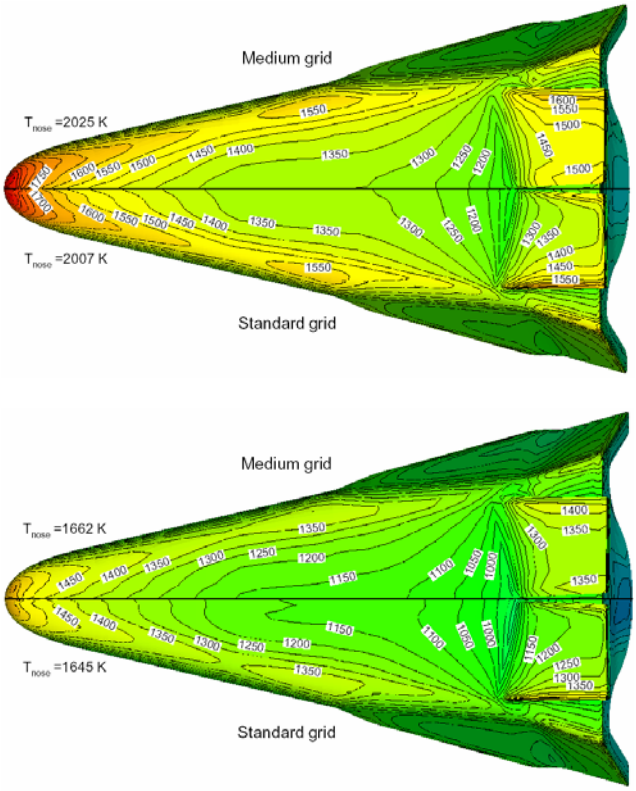

Fig. 8: Surface temperature distribution for Ma=24.5 assuming partially catalytic walls. Top: SPHYNX, bottom: X-38.

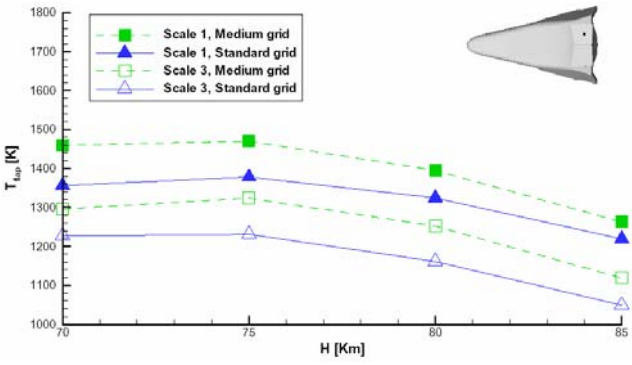

Fig. 9: Evolution of the flap windward side temperature as a function of grid density and flight altitude for both vehicles: SPHYNX (scale 1) and X-38 (scale 3).

The present study provides the opportunity to examine the possibility whether one can take advantage of an existing aerodynamic and/or aerothermodynamic database (ADB and/or ATDB respectively) to design a downsized or upsized vehicle which could fly also a different trajectory. That is, the SPHYNX situation departing from X-38 but also a more realistic future scenario, taking advantage of an existing database for a small demonstrator to design the corresponding operational vehicle accounting not only for differences in size but also on flight trajectory. As the SPHYNX concept is based on a subscale model, its trajectory can be anticipated to be different from that of the X38. Indeed, **Fig. 10** shows the differences in re-entry trajectory between X-38 and SPHYNX. Thus, despite the availability of an aerothermodynamic database compiled to be compatible with the X38 shape and mission, the question arises whether it could be possible or not to use such a valuable amount of data to asses the feasibility of the SPHYNX concept itself.

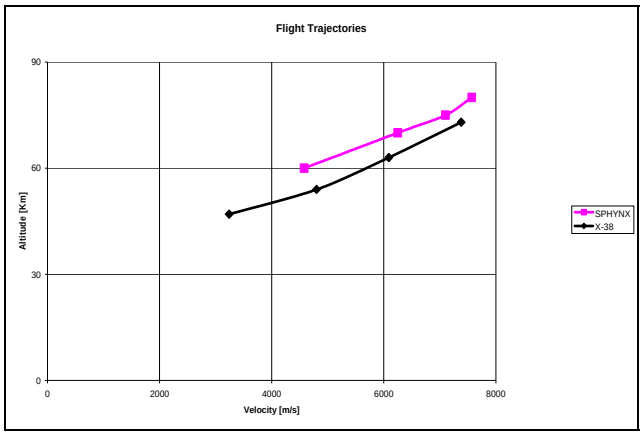

Fig. 10: Re-entry trajectories considered

For an aerodynamic database the Reynolds number is the first choice for a similarity parameter since the variables to be considered are from the point of view of the trajectory, flight speed and flight altitude; from the point of view of the geometry only the size of the vehicle. All they are included in the Reynolds number (Re). Furthermore, here only coefficients for lift (CL), drag (CD) and pitching moment (Cm) are considered since the available information for the lateral derivatives of the X-38 and SPHYNX vehicle is too poor to establish any conclusion. **Figures 11-13** present the case of the SPHYNX design based on the existing X-38 aerodynamic database. The figures show the X-38 aerodynamic database maximum uncertainty margins [7], the past computed CFD values for X-38 and the here obtained values for SPHYNX.

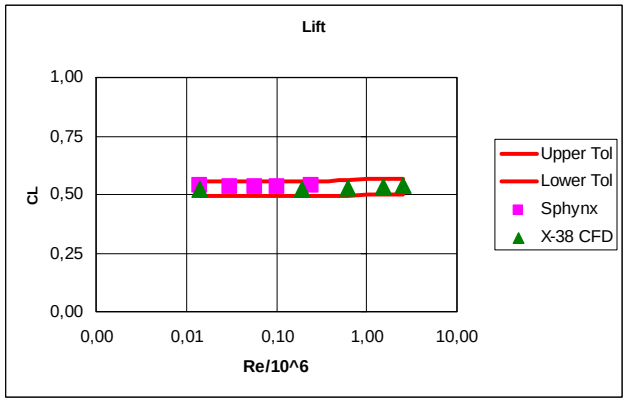

Fig. 11: Lift coefficient evolution with Reynolds number.

The X-38 aerodynamic database and its associated margins are based on wind tunnel and CFD results from different sources. The uncertainty data consist

of increments or percentage variations in the important aerodynamic coefficients and derivatives as a function of Mach number along a nominal trajectory. The control laws would need to be able to handle these errors with little or no effect on the vehicle stability or guidance. In particular wind tunnel data were used to define an appropriate uncertainty magnitude in the subsonic and supersonic flight regions, while for the hypersonic Mach numbers, the uncertainty model was based on comparisons of wind-tunnel and analysis code predictions of vehicle aerodynamics documented during the program. Furthermore, to establish the hypersonic uncertainties, a distinction was made between two notions: the "tolerances", i.e. the uncertainty in the assessment of the aerodynamic coefficients, and the "variations", i.e. the uncertainties in the extrapolation to flight conditions.

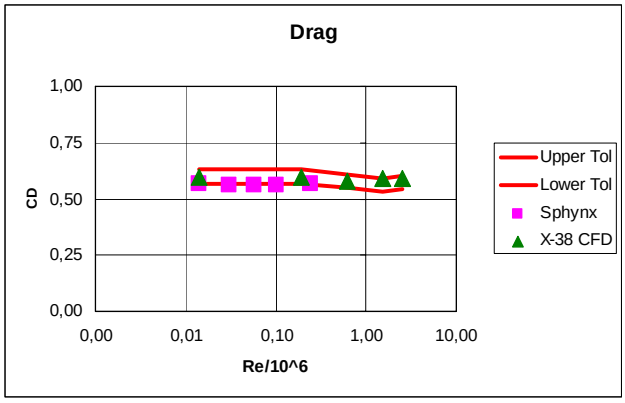

Fig. 12: Drag coefficient evolution with Reynolds number.

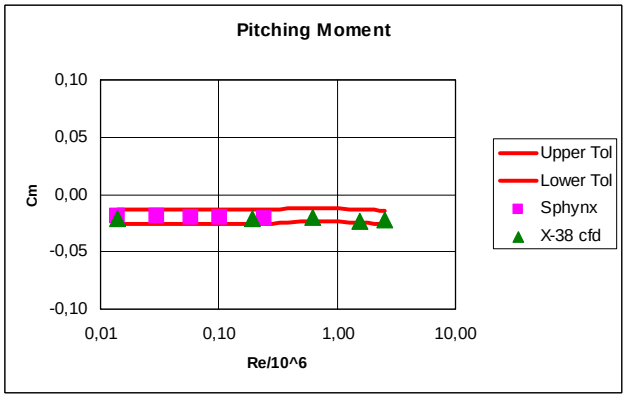

Fig. 13: Pitching moment coefficient evolution with Reynolds number.

The Figures shown that the computed values for SPHYNX fit very well inside the uncertainty band of the X-38 aerodynamic database. Furthermore, the observed discrepancies are not larger than the resulting differences between the computed values for X-38 and the X-38 uncertainty band. Also, the aerodynamic coefficients here analyzed are almost Reynolds number independent. The figures clearly demonstrate that one could aerodynamically design a down sized vehicle using an existing aerodynamic database for a similar but larger vehicle shape even when both fly different trajectories.

For an aerothermodynamic database the classic viscous interaction parameter done by the Mach number divided by the square root of the Reynolds number, i.e. a quantity characteristic for the boundary layer thickness, is selected as similarity parameter. The heat loads are here presented through the heat flux coefficient (CH), i.e. heat loads divided by flight density and flight velocity to the third power. Heat fluxes are taken at three different locations, the stagnation point, and one arbitrary location at the leeward and at the windward side. In addition, since the aerothermodynamic database for X-38 contains only very few results for partial catalytic walls, the present analysis is conducted using only fully catalytic solutions. **Figures 14-16** demonstrate the feasibility of applying an existing aerothermodynamic database to design a down sized vehicle that flies also a different trajectory. The results are scaled logarithmic for both axes. For this scaling they show linear behavior all over the trajectory and especially for all investigated positions on the surface.

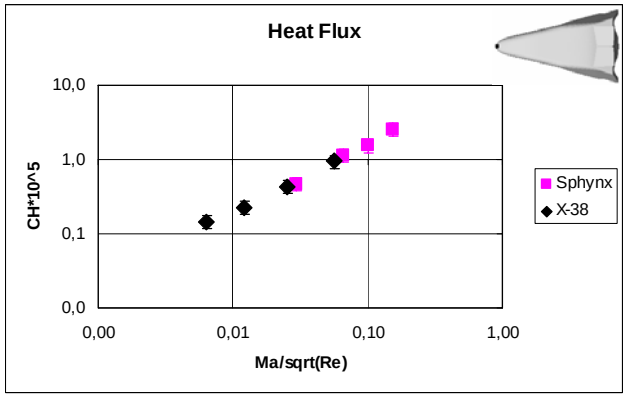

Fig. 14: Stagnation point heat flux evolution with Reynolds number.

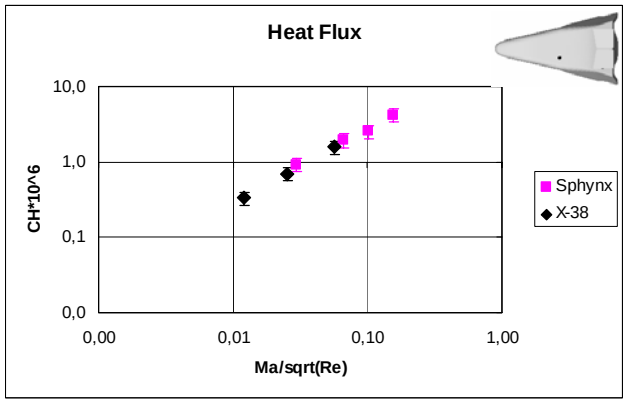

Fig. 15: Windward side heat flux evolution with Reynolds number (position taken from Fig. 6).

CONCLUSIONS

The present study summarized the DLR contribution to the ESA study for a small re-entry demonstrator. The vehicle, called SPHYNX (Subscale Precursor HYpersoNic X vehicle), has the shape of the X-38 lifting body scaled to 33% and therefore makes use of the well-known aerodynamic and aero-thermodynamic behavior of the X-38.

The current aero- and aero-thermodynamic study has been carried out based on the solutions of the stationary Navier-Stokes equations. Several flow conditions derived from the flight trajectory have been considered, in particular the portion comprised from 85 Km to 60 Km altitudes, i.e. Mach numbers from 28 to 14. All Navier-Stokes simulations have been carried out for chemical non-equilibrium under laminar flow conditions. Fully and partially catalytic wall conditions have been considered. The numerical results have been assessed by grid convergence studies and by comparing the present results with available results for the X-38 vehicle. Heat fluxes, thermal loads and aerodynamic coefficients for aileron and flap deflections compare rather well with former studies for the X-38.

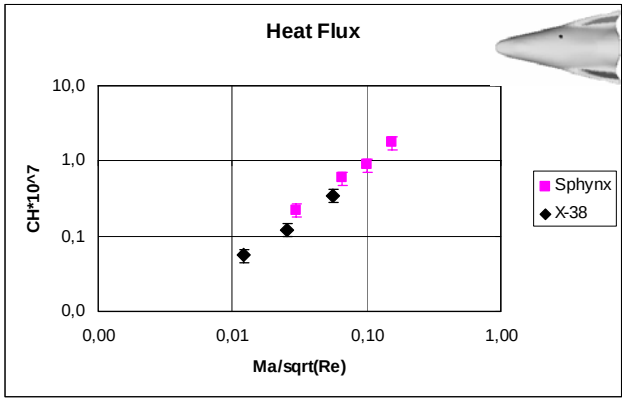

Fig. 16: Leeward side heat flux evolution with Reynolds number (Position taken from Fig. 7).

The present study provides first evidences about the possibility to use an existing aerodynamic and/or aerothermodynamic database to design a downsized or upsized vehicle which fly a different re-entry trajectories. That is, the SPHYNX situation departing from X-38 but also a more realistic future scenario, taking advantage of an existing database for a small demonstrator to design the corresponding operational vehicle accounting not only for differences in size but also on flight trajectory. From an aerodynamic point of view, the study covers with sufficient evidence the longitudinal motion. Further studies should be performed to assess the lateral motion. From an aerothermodynamic point of view, the present investigation is valid only for thermal data obtained under laminar non-equilibrium flow, fully catalytic wall conditions. The present investigation should be completed considering turbulent non-equilibrium conditions as well as non-catalytic wall conditions for laminar and turbulent flows.

In spite of the previous remarks and in view to the future European Programs, the here presented results are very promising. Regarding that the development of, in particular, an aerodynamic database but also an aerothermodynamic database have a large impact in the vehicle development costs (the aerodynamic data base of the US-Orbiter required among others 27000 hours of wind tunnel!) and that a sub-scaled demonstrator is always more accessible in terms of budget than a full size one, the present study confirms the large potential of a sub-scaled demonstrator strategy.

ACKNOWLEDGMENT

The present investigation has been carried out by DLR in the frame of the ESA-Contract No. 17256/03/NL/PA, “Contribution of DLR to the Aerodynamic Data Base of the SPHYNX Re-entry vehicle”.

REFERENCES

[1] Püttmann, N.; Brücker, H.; Dittmann, R., Noack, E.; “TETRA& ASTRA – Milestones on the road to new technologies for future space transportation systems”; Proceedings of the International Astronautical Conference 2000, Paper IAF-00-V.04, 2000.

[2] Graf, E.D.; “The X-38 and Crew Return Vehicle Programmes”; ESA Bulletin 101, February 2000.

[3] Hilfer, C.; “X-38 Full scale TPS qualification”, Proceedings of the Internat.l Astronautical Conference 2002; Paper IAC-02-V.5.06, 2002.

[4] Radespiel, R.; Longo, J.M.A.; Brück,S.; Schwamborn, D.; “Efficient numerical simulation of Complex 3D Flows with Large Contrast”; AGARD-FDP Symposium on Progress and Challenges in CFD Methods and Algorithms, AGARD CP-578, 1996, pp 33-1 to 33-11.

[5] Bergemann, F.; “Gaskinetische Simulation von kontinuumsnahen Hyperschall-strömungen unter Berücksichtigung von Wandkatalyse”; DLR-FB 94-30, 1994, Göttingen.

[6] Brück, S.; “Ein Beitrag zur Beschreibung der Wechselwirkung von Stößen in reaktiven Hyperschallströmungen”; DLR-FB 98-06, 1998, Göttingen.

[7] Longo, J.M.A.; Lüdeke, H.; Brück, S.; Orlowski, M.; Rapuc, M.; Tribot J.-P.; Stojanowski, M.; “X-38: A Test Bed For The CEVCATS-N Code”; AAAF, Proceedings of the First International Symposium on Atmospheric Reentry Vehicles and Systems, Arcachon, France, 1999.

[8] Brodersen, O.; Hepperle, M.; Ronzheimer, A.; Rossow, C.-C.; Schöning, B.; “The Parametric Grid Generation System MegaCads”; Proceedings of the 5th International Conference on Numerical Grid Generation in Computational Field Simulation, NSF Mississippi State, 1996, pp 353 to 362.